ECCOMAS Congress 2016
VII European Congress on Computational Methods in Applied Sciences and Engineering
M. Papadrakakis, V. Papadopoulos, G. Stefanou, V. Plevris (eds.)
Crete Island, Greece, 5–10 June 2016

THE XFEM FOR A SIMPLIFIED MODEL IN HYDRAULIC FRACTURING

Markus Schätzer[1], **Thomas-Peter Fries**[1]

[1]Institute of Structural Analysis, Graz University of Technology
Lessingstr. 25/II, 8010 Graz, Austria
e-mail: {schaetzer, fries}@tugraz.at

Keywords: energy release rate, stress intensity factors, superposition, crack opening displacements.

Abstract. *Hydraulic fracturing is an important branch in geomechanics, where a fracture initiates and propagates in the host rock due to the induced hydraulic loading. The pressure exerted by the fracking fluid onto the surrounding solid, typically is obtained by a Reynolds equation which relates the crack width with the pressure. This poses severe difficulties for the numerical treatment, also in terms of robustness. In the presented work, the Reynolds equation is replaced by pre-defined pressure distributions which leads to a much simpler and robust coupled problem. For each assumed distribution, the critical pressure is determined where the critical energy release rate G_c is exceeded. The influence of the different distributions is investigated in a separate example. The energy release rates are determined based on stress intensity factors with the XFEM by using crack opening displacements. This happens by a comparison of an approximated state which represents the computed displacements in the solid, and a reference state which represents the expected openings for a pure mode I, II and III. This method is intuitive, computationally cheap and has the advantage that only displacements are fitted, wherefore no additional consideration of pressurized crack surfaces is required.*

The critical pressure is determined based on the superposition principle in linear elastic fracture mechanics. Herein, a separate observation of the external loadings by means of volume forces and tractions at the boundary, and the internal loadings by means of the pressure exerted by the fracking fluid is done. Based on a scaling factor of the internal state, the critical pressure is extracted from the energy release rate.

1 Introduction

Hydraulic fracturing is a standard procedure for the stimulation of petroleum and geothermal reservoirs. A fluid is pumped into the solid until a fracture initiates and propagates. For the modelling, three important factors have to be considered: (*i*) the pressure exerted by the fracking fluid onto the surrounding solid, (*ii*) the deformation of the solid and the associated fracture volume, and (*iii*) the propagation of crack surfaces.

In general, the pressure induced by the fracking fluid is obtained by a Reynolds equation [1] which relates the pressure with the crack width. That is, several iterations between field (*i*) and (*ii*) are necessary, which is not always robust and leads to a complex behaviour at the crack tip/front (toughness or viscous regimes [2]). This contribution deals with a simplified model where the Reynolds equation is replaced by pre-defined pressure distributions which are scaled by only few parameters. This assumption leads to a much simpler and robust coupled problem. It is noted that only polynomial pressure distributions, depending on the distance r to the crack tip/front and an initial pressure value p_0 are considered in this contribution as shown in Section 4.2. The introduced method is not limited on this restricted group of functions and treats all pressure distributions in the same manner.

Many numerical methods exist for solving the linear elastic fracture problem, however, most of them such as the standard finite element method (FEM) and the boundary element method (BEM) have a limited efficiency due to the $\sqrt{r}$ behaviour of the displacements in the vicinity of the crack tip/front. The use of special elements, like 'quarter-point' elements [3, 4, 5], improves the approach, but a suitable mesh has to be provided for each crack geometry during propagation which frequently requires a remeshing. An optimal accuracy on *fixed* meshes is possible with the extended finite element method (XFEM) [6] which treats non-smooth solution features within elements by additional enrichment functions. In this method, the localisation of the non-smooth features or in the context of linear elastic fracture mechanics the localisation of the crack path/surface is often done by the use of level-set functions [7, 8]. However, the update of these functions after a propagation step can be cumbersome [8], wherefore in [9] a hybrid explicit-implicit crack description is used which combines the advantages of the level-set functions with those of an explicit crack description, e.g. by means of straight line segments or flat triangles. This crack representation allows a simple update of the crack geometry during the crack propagation, wherefore it is used in this work.

In the third field (*iii*), it is determined whether the crack propagates and in which direction. The maximum circumferential stress criterion is often employed, where the crack propagates in direction of the maximum circumferential stresses when a critical energy release rate G_c is reached [6]. In linear elastic fracture mechanics, the current energy release rate G is often evaluated by the J-integral [10] as they are equivalent [11]. The direction of the propagation is often determined by stress intensity factors (SIFs) which are also related to G [12].The interaction integral is one of the most important technique for the computation of SIFs, however the evaluation of this integral can be cumbersome for complex three-dimensional crack configurations. In this work, SIFs are determined by observing the displacement field, particularly the crack opening displacements (CODs), in the vicinity of the crack tip/front and their comparison with the expected openings for a pure mode *I*, *II* and *III* crack.

The focus of this contribution is the evaluation of critical pressure values p_c for assumed pressure distributions on mixed-mode loaded crack configurations. This examination is the first step towards a simplified hydraulic fracturing model.

2 Computation of SIFs by using CODs in XFEM

In this section, the XFEM approach in linear elastic fracture mechanics with a hybrid explicit-implicit crack description and the computation of stress intensity factors (SIFs) by crack opening displacements is shortly recalled.

The XFEM extends the standard finite element method (FEM) approach by additional enrichment functions which involve non-smooth features within elements with optimal accuracy. A *priori* knowledge about the non-smooth solution characteristics is essential for the enrichment functions. In linear elastic fracture mechanics, a domain Ω is cracked by the (curved) crack path/surface Γ_c. The displacements are discontinuous along Γ_c and the stresses are singular at the crack tip/surface and the following enriched approximation has proven useful [6]

$$u^h(\mathbf{x}) = \sum_I N_i(\mathbf{x}) u_i + \sum_{I^*} N_i(\mathbf{x}) \psi_{step}(\mathbf{x}) a_i + \sum_{j=1}^{4} \sum_{J^*} N_i(\mathbf{x}) \psi_{tip}^j(r,\theta) b_i^j. \tag{1}$$

Herein, ψ_{step} considers discontinuous displacements along the crack path/surface and ψ_{tip} the singular stresses at the crack tip/front. N_i are the finite element shape functions, a_i and b_i^j additional degrees of freedom at the enriched nodes I^* and J^*. It is standard to use the Heaviside function for the step enrichment ψ_{step} [6] and

$$\psi_{tip}^j(r,\theta) = \left[\sqrt{r} sin\frac{\theta}{2},\ \sqrt{r} cos\frac{\theta}{2},\ \sqrt{r} sin\frac{\theta}{2} sin\theta,\ \sqrt{r} cos\frac{\theta}{2} sin\theta \right] \tag{2}$$

for the crack tip/front enrichment. These enrichment functions are based on a polar coordinate system (r,θ) which has its origin at the crack tip/front and is aligned with the tangent at the crack tip/front. Typically, the localisation of the crack geometry and the determination of the polar coordinate system is based on level-set functions. In [9] a hybrid explicit-implicit crack description has been introduced which allows a simple update of the level-sets during propagation. Herein, three level-set functions are defined as follows:

- $\phi_1(\mathbf{x})$ is the (unsigned) distance function to the crack path/surface.
- $\phi_2(\mathbf{x})$ is the (unsigned) distance function to the crack tip/front.
- $\phi_3(\mathbf{x})$ is a signed distance function to the extended crack path/surface.

These definitions extend straightforward also to three dimensions and imply the polar coordinate system (r,θ) which is used for the enrichment functions, and a local coordinate system (a,b) which is used for the computation of SIFs. Further details of the different coordinate systems are given in [9]. In the following, the evaluation of SIFs by crack opening displacements (CODs) is discussed.

2.1 Computation of SIFs

The proposed method offers an intuitive and computationally cheap technique for the evaluation of SIFs which treats three dimensional crack configurations in the same manner as two dimensional ones. Furthermore, no modification is necessary for curved and loaded crack surfaces. The use of CODs has the advantage that translations by means of rigid body motions are considered automatically. SIFs are computed by a comparison of CODs of an approximated

state by means of the XFEM solution and a reference state which represents the expected openings for a pure mode *I*, *II* and *III* crack. The following paragraph shows the main idea of the proposed method.

The approximated CODs are determined by Eq. 1 as a post-process step. The difficulty here is that the enrichment and shape functions have to be evaluated in a special setting so that CODs are obtained. For that, in a first step a point has to be found on the implicitly defined crack path/surface. As level-set values are only given in the nodes and are interpolated within the elements by the corresponding shape functions, curved zero level-sets are present in general. This complicates the finding of points with zero level-set values within the elements. Therefore, each potentially cut element, identified by the condition

$$max[\phi_3(\mathbf{x}_i)] \cdot min[\phi_3(\mathbf{x}_i)] < 0, \tag{3}$$

is subdivided into two linear triangular elements in two dimensions or six linear tetrahedral elements in three dimensions, which enable a simple detection of zero level-sets as they are piecewise linear/planar within these simplex elements. A similar setting is used for linear elements in [13, 14] and for higher order elements in [15]. As the enrichment functions and displacements are discontinuous along the zero level-sets the point has to be *splitted* into two opposite but infinitesimally close points of the crack path/surface. This splitting is done in the simplex elements based on the normal vector of the zero level-set. Then the global crack opening displacement $\Delta\mathbf{u}^h_{\mathbf{x}}(S)$ by means of the global coordinate system (x,y,z) of the point S is evaluated by Eq. 1.

The expected crack opening displacement $\Delta\mathbf{u}^m_{\mathbf{a}}(S)$ of the point S and mode m is evaluated in the (a,b,c)-coordinate system by the governing equations of linear elastic fracture mechanics based on stress intensity factors [16] where, successively, one SIF k_m is set to 1 and the others to 0.

A comparison of these two states leads to the SIFs. As both CODs have to be in the same coordinate system, the approximated CODs are transformed into the (a,b,c)-coordinate system based on the Jacobi-matrix $\mathbf{J}$ as shown in Eq. 4. Herein, the partial derivatives of the third function c are determined by the cross product of ∇a and ∇b.

$$\Delta\mathbf{u}^h_{\mathbf{a}} = \mathbf{J} \cdot \Delta\mathbf{u}^h_{\mathbf{x}} \qquad \text{with} \quad \mathbf{J} = \begin{bmatrix} a_{,x} & a_{,y} & a_{,z} \\ b_{,x} & b_{,y} & b_{,z} \\ c_{,x} & c_{,y} & c_{,z} \end{bmatrix}, \quad i = 1,2,3. \tag{4}$$

It has been shown, for example, in [16] that each stress intensity factor k_m has a preferred direction with the highest impact on the associated displacements. Taking these directions into account, the SIFs can be directly computed by

$$k_I = \Delta u^h_b / \Delta u^I_b, \qquad k_{II} = \Delta u^h_a / \Delta u^{II}_a, \qquad k_{III} = \Delta u^h_c / \Delta u^{III}_c. \tag{5}$$

This fitting method is the basis for the further work, as all needed SIFs are evaluated by it. In the following section, the evaluation of critical pressure values for a general mixed-mode loaded crack configuration is discussed.

3 Evaluation of critical pressure values

In hydraulic fracturing, a fluid is pumped into the solid until a fracture initiates and propagates. The fracture propagates when a critical value of the energy release rate G is reached. That is, the crack propagates if the following equation is fulfilled

$$G \geq G_c. \tag{6}$$

The current energy release rate G is obtained by the associated SIFs which are evaluated by the proposed method presented in Section 2.1 and their relation to G. For a general three dimensional mixed-mode loading and the assumption that mode *II* and *III* are small compared to mode *I* which leads to a *quasi planar* crack propagation, the energy release rate is given by [12] as follows:

$$G(k_m) = \frac{\left(1-\nu^2\right)}{E}\left(k_I^2 + k_{II}^2\right) + \frac{1}{2\mu}k_{III}^2. \tag{7}$$

Herein, k_m are the current SIFs, ν the Poisson's ratio and μ the second Lamé-Constant. It is noted that this representation of G is used for simplicity. The proposed method is not limited to it, wherefore also formulations of infinitesimally kinked crack extensions [16, 17] are possible which will be considered in future works.

In general, the pressure exerted by the fracking fluid onto the surrounding solid is obtained by a Reynolds equation which relates the crack width with the pressure. In this contribution, the model is simplified as the Reynolds equation is replaced by pre-defined pressure distributions which are scaled by the initial value p_0 and the crack length l_c as shown in Section 4.2. One may distinguish two different types of loadings in hydraulic fracturing. The first is called *'external'* and contains body forces, prescribed tractions at the boundary Γ_t and prescribed displacements at the boundary Γ_u. The second type of forces is called *'internal'* and contains the pressure exerted by the fracking fluid onto the surrounding solid. For the second type it is also demanded that the displacements at Γ_u are zero. An illustration of a cracked domain, where both loading types are shown is given in Fig. 1(a).

In most practical applications of hydraulic fracturing, the interest is based on the computation of a critical pressure p_c which causes a propagation of the crack. Hence, this contribution deals with the evaluation of critical pressures for pre-defined distributions. In linear elastic fracture mechanics, there holds for a unit prescribed pressure distribution p_0 without external loadings that their associated SIFs scale proportionally with

$$k_m^p(\lambda \cdot p_0) = \lambda \cdot k_m^p(p_0). \tag{8}$$

Herein, the index p indicates that the SIFs are obtained due to pure internal loadings. A differentiation of the SIFs due to internal and external loadings is needed at a later point of this work. Eq. 8 plugged into Eq. 7 and Eq. 6 leads to the critical pressure p_c as

$$p_c = \lambda \cdot p_0 \qquad \text{with}: \quad \lambda = \sqrt{\frac{G_c}{G\left(k_m^p(p_0)\right)}}. \tag{9}$$

Eq. 9 is only valid for pure internal loadings, as an increase of the pressure level does not influence the crack behaviour or energy release rate G caused by the external loadings. Therefore, a separate observation of the crack behaviour caused by the external and internal loadings is necessary. In linear elastic fracture mechanics, this is achieved by using the superposition principle as shown in Fig. 1. Herein, the crack configuration is decoupled into a part with only external loadings and a part with only internal loadings. The associated SIFs are denoted by k_m^{ext} for the external case, k_m^p for the internal case and k_m^{total} for the combined case. If a λ-scaled unit pressure distribution p_0 is assumed, Eq. 8 holds for the internal part. The total SIFs k_m^{total} are given by the sum of the external and internal case.

$$k_m^{total} = k_m^{ext} + \lambda k_m^p. \tag{10}$$

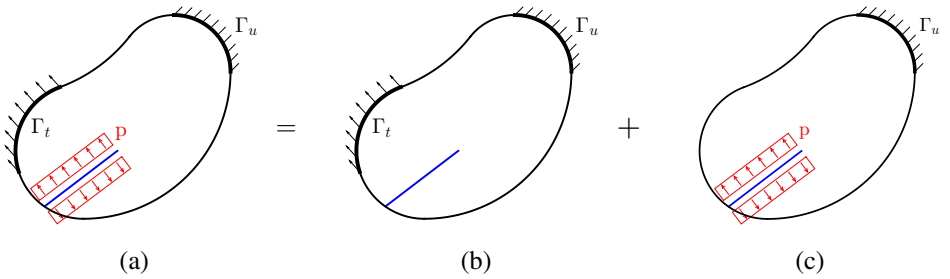

Figure 1: Superposition of an externally and internally loaded crack by means of the principle of superposition. (a) Totally loaded, (b) externally loaded and (c) internally loaded.

Eq. 10 plugged into Eq. 7 and Eq. 6 leads to a quadratic equation of λ as it holds for the principle of superposition applied to the energy release rate G_m of mode m

$$G_m = \left(\sqrt{G_m^{ext}} + \sqrt{G_m^{p}}\right)^2. \tag{11}$$

That is, for the computation of λ, coupled terms of the external and internal state are involved. The quadratic equation for λ can be expressed as follows:

$$\begin{aligned} 0 = a\lambda^2 + b\lambda + c \qquad \text{with} \quad & a = G(k_m^p), \\ & b = \frac{2(1-\nu^2)}{E}\left(k_I^{ext}k_I^p + k_{II}^{ext}k_{II}^p\right) + \frac{1}{\mu}k_{III}^{ext}k_{III}^p, \\ & c = G(k_m^{ext}) - G_c. \end{aligned} \tag{12}$$

It is noted that only one value of λ ($\lambda \geq 0$) leads to a physically reasonable critical pressure. This is checked by the criterion

$$\lambda_1\lambda_2 > 0 \qquad \text{for} \quad \lambda_1 \neq \lambda_2. \tag{13}$$

The evaluated λ leads to the critical pressure p_c by Eq. 9. In the following section, first results of the proposed simplified model for hydraulic fracturing are presented in two dimensions.

4 Numerical examples

In this section two different things are investigated in two dimensions. Firstly, how the critical pressure value due to a constant pressure distribution is changed for a given mixed-loaded crack configuration relating to the crack length. Furthermore, how the crack propagates by the presented critical pressure and external loading. Secondly, how the pressure distribution influences the critical pressure. For the investigation of these two points an edge cracked rectangular plate with the extent of $h = 7\,\text{m}$, $l = 16\,\text{m}$ and an initial crack length $l_c = 3.5\,\text{m}$ is used as shown in Fig. 2(a). The plate is clamped on the left side and is described by 4-node bilinear quadrilateral elements with different mesh sizes. A brittle and isotropic material is used with a Youngs modulus $E = 35\,\text{GPa}$, a Poissons ratio $\nu = 0.3$ and a critical energy release rate $G_c = 1\,\text{J}/\text{m}^2$. Furthermore, plane stress conditions are assumed. Obviously, the chosen setup is not really related to a problem in geomechanics. Nevertheless, the approach is general enough that it is also working in the context of plates where we find more general loading conditions such as those dominated by shear. The interest is only based on the computation of critical pressure values for a given pressure distribution, wherefore no dynamic effectes [18], cohesive models [19] or viscosity-dominated regimes [20] are considered.

4.1 Mixed-mode loaded crack configuration

At first the change of the critical pressure during a crack propagation of a mixed-mode loaded crack configuration is investigated. For that, the plate is loaded by a shear traction $\tau = 1\,\mathrm{kN/m}$ on the right side and a constant pressure within the fracture as shown in Fig. 2(a). Herein, the

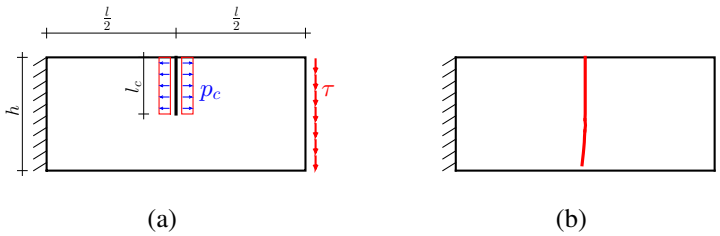

Figure 2: Mixed-loaded crack configuration: (a) Situation and (b) crack propagation.

external loading τ leads to a mixed-mode behaviour at the crack tip, whereas the internal loading only represents a mode I crack. For each propagation step the critical pressure is evaluated by the introduced method, which leads to a propagation of the crack. Based on the maximum circumferential stress criterion, the propagation angle θ_c can be expressed by the SIFs as follows [6]:

$$\theta_c = 2arctan\frac{1}{4}\left(\frac{k_I}{k_{II}} \pm \sqrt{\left(\frac{k_I}{k_{II}}\right)^2 + 8}\right), \tag{14}$$

where the sign depends on the sign of k_{II}. For the considered example, it is assumed that the crack propagates with the increment $\Delta a = 0.35\,\mathrm{m}$ in direction of θ_c. The required pressure for the propagation is illustrated in Fig. 3, where the critical pressure is plotted over the current crack length. Herein, seven different meshes are used with an element number from 9,401 to 46,025.

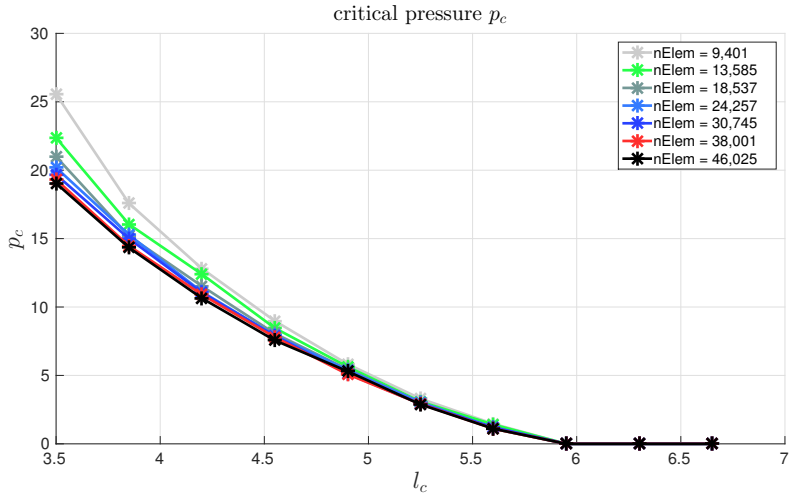

Figure 3: Critical pressures during the crack propagations.

As expected the pressure which is needed for the propagation decreases with an increasing crack length and becomes zero if a critical crack length is reached, which means that the crack propagates only by the external loading. The results also show a convergence to a fixed value.

The resulting crack path is illustrated in Fig. 2(b). At the beginning the crack propagates almost straight as the internal loading is dominant. However, at the end very low or zero pressures already leads to a propagation, wherefore the influence of the external loading increases which leads to a deviation of the straight crack path.

4.2 Different pressure distributions

In this example the influence of different pressure distributions are investigated. Herein, the plate of Section 4.1 is used again. The focus is based on the influence of the pressure distribution, wherefore only a *static* crack configuration without any external loadings is investigated. Three different distributions are considered which only depend on the distance r to the crack tip and the initial pressure p_0 as shown in Fig. 4.

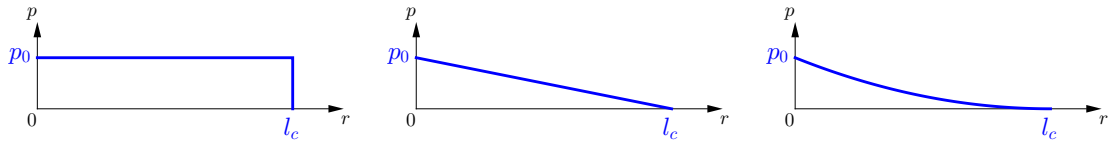

Figure 4: Different pressure distributions: (a) Constant, (b) linear and (c) quadratic.

It is noted that the introduced method is not limited on these distributions, however they allow an easy introduction into the complex topic of hydraulic fracturing. These distributions are used as internal loading of the rectangular plate which was introduced in Section each distribution on different meshes. The results are illustrated in Fig. 5 where the relation of the resulting pressure force R_c and the crack length l_c is plotted over the element number. R_c is illustrated instead of p_0 to take account of the fact that linear or quadratic distributions have a lower resulting force. The results show as expected that concentrations of the pressure at the crack tip lead to a higher

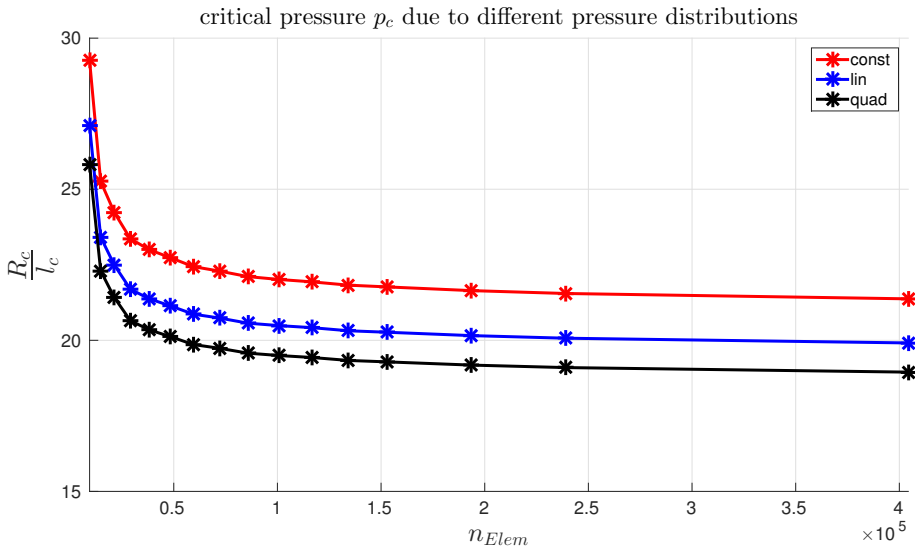

Figure 5: Critical pressures for different pressure distributions.

loading of the fracture, wherefore a lower pressure is needed for the propagation. All results of the considered pressure distributions converge similar.

5 Conclusion

In the presented work, a simplified hydraulic fracturing model by means of pre-defined pressure distributions instead of using the Reynolds equation is investigated. These distributions are scaled by only a few parameters, which results in a much simpler and robust coupled problem. The influence of the distributions is investigated in a numerical study. Critical pressure values are evaluated based on the superposition principle of linear elastic fracture mechanics, where the influence of the external and internal loadings is observed separately and scaled by a factor. This critical pressure leads to a propagation of the crack in direction of the maximum circumferential stresses.

The deformations of the solid are solved by an XFEM simulation with a hybrid explicit-implicit crack description which allows a simple update of the crack geometry during a propagation. Based on the deformations, particularly crack opening displacements (CODs), SIFs and energy release rates are computed by a comparison of the approximated and reference states. This method provides an intuitive, computationally cheap and robust method, which works in two dimensions as well as in three dimensions in a consistent manner.

Numerical results show the relation of the critical pressure value and the crack length. The influence of the pressure distributions is investigated in an own example. As all considered examples are in good agreement with the expected solutions and converge to a fixed value it is concluded that the proposed simplified hydraulic fracturing model provides a simple and robust basis for further investigations.

REFERENCES

[1] J. Adachi, E. Siebrits, A. Peirce, and J. Desroches, Computer simulation of hydraulic fractures. *Rock Mechanics & Mining Sciences*, **44**, 739–757, 2007.

[2] A. Peirce, Modeling multi-scale processes in hydraulic fracture propagation using the implicit level set algorithm. *Comput. Methods Appl. Mech. Engrg.*, **283**, 881–908, 2015.

[3] L.J. Gray, A.-V. Phan, G.H. Paulino, and T. Kaplan, Improved quarter-point crack tip element. *Eng. Fract. Mech.*, **70**, 269–283, 2003.

[4] G.P. Nikishkov, Accuracy of Quarter-point Element in Modeling Crack-tip Fields. *CMES-Computer Modeling In Engineering & Sciences*, **93**, 335–361, 2013.

[5] M. Nejati, A. Paluszny, and R.W. Zimmerman, On the use of quarter-point tetrahedral finite elements in linear elastic fracture mechanics. *Eng. Fract. Mech.*, **144**, 194–221, 2015.

[6] N. Moës, J. Dolbow, and T. Belytschko, A finite element method for crack growth without remeshing. *Internat. J. Numer. Methods Engrg.*, **46**, 131–150, 1999.

[7] M. Stolarska, D.L. Chopp, N. Moës, and T. Belytschko, Modelling crack growth by level sets in the extended finite element method. *Internat. J. Numer. Methods Engrg.*, **51**, 943–960, 2001.

[8] A. Gravouil, N. Moës, and T. Belytschko, Non-planar 3D crack growth by the extended finite element and level sets - Part II: Level set update. *Internat. J. Numer. Methods Engrg.*, **53**, 2569–2586, 2002.

[9] T.P. Fries, M. Baydoun, Crack propagation with the extended finite element method and a hybrid explicit-implicit crack description. *Internat. J. Numer. Methods Engrg.*, **89**, 1527–1558, 2012.

[10] J.R. Rice, A Path Independent Integral and the Approximate Analysis of Strain Concentration by Notches and Cracks. *J. Appl. Mech.*, **35**, 379–386, 1968.

[11] M.F. Kanninen, C.H. Popelar, Advanced fracture mechanics. *Oxford University Press*, 1985.

[12] N. Moës, A. Gravouil, and T. Belytschko, Non-planar 3D crack growth by the extended finite element and level sets - Part I: Mechanical model. *Internat. J. Numer. Methods Engrg.*, **53**, 2549–2568, 2002.

[13] T.P. Fries, A corrected XFEM approximation without problems in blending elements. *Internat. J. Numer. Methods Engrg.*, **75**, 503–532, 2008.

[14] T.P. Fries, T. Belytschko, The extended/generalized finite element method:An overview of the method and its applications. *Internat. J. Numer. Methods Engrg.*, **84**, 253–304, 2010.

[15] T.P. Fries, S. Omerović, Higher-order accurate integration of implicit geometries. *Internat. J. Numer. Methods Engrg.*, early view.

[16] T.L Anderson, Fracture mechanics: fundamentals and applications. *CRC Press*, 2005.

[17] H. Awaji, T. Kato, S. Honda, and T. Nishikawa, Criterion for combined mode I-II of brittle fracture. *J. Ceram. Soc. Japan*, **107**, 918–924, 1999.

[18] D. Haboussa, D. Grégoire, T. Elguedj, H. Maigre, and A. Combescure, X-FEM analysis of the effects of holes or other cracks on dynamic crack propagations. *Internat. J. Numer. Methods Engrg.*, **86**, 618–636, 2011.

[19] N. Moës, T. Belytschko, Extended finite element method for cohesive crack growth. *Eng. Fract. Mech.*, **69**, 813–833, 2002.

[20] A. Peirce, E. Detournay, An implicit level set method for modeling hydraulically driven fractures. *Comp. Methods Appl. Mech. Engrg.*, **197**, 2858–2885, 2008.